Opposing impact of B cell intrinsic TLR7 and TLR9 signals on autoantibody repertoire and systemic inflammation

Shaun W. Jackson[*,¶], **Nicole E. Scharping**[¶], **Nikita S. Kolhatkar**[†,¶], **Socheath Khim**[¶], **Marc A. Schwartz**[†,¶], **Quan-Zhen Li**[#], **Kelly L. Hudkins**[‡], **Charles E. Alpers**[‡], **Denny Liggitt**[§], and **David J. Rawlings**[*,†,¶]

[*]Department of Pediatrics, University of Washington School of Medicine

[†]Department of Immunology, University of Washington School of Medicine

[‡]Department of Pathology, University of Washington School of Medicine

[§]Department of Comparative Medicine, University of Washington School of Medicine

[¶]Seattle Children's Research Institute, Seattle, WA

[#]Department of Immunology, University of Texas Southwestern Medical Center, Dallas, TX

Abstract

Systemic lupus erythematosus (SLE) is a multisystem autoimmune disease characterized by autoantibodies targeting nucleic acid-associated antigens. The endosomal toll-like receptors TLR7 and TLR9 are critical for generation of Abs targeting RNA- or DNA-associated antigens, respectively. In murine lupus models, deletion of TLR7 limits autoimmune inflammation, while deletion of TLR9 exacerbates disease. Whether B cell or myeloid TLR7/TLR9 signaling is responsible for these effects has not been fully addressed. Here, we utilize a chimeric strategy to evaluate the effect of B cell-intrinsic deletion of TLR7 vs. TLR9 in parallel lupus models. We demonstrate that B cell-intrinsic TLR7 deletion prevents RNA-associated Ab formation, decreases production of class-switched Abs targeting non-nuclear antigens and limits systemic autoimmunity. In contrast, B cell-intrinsic TLR9 deletion results in decreased DNA-reactive Ab, but increased Abs targeting a broad range of systemic autoantigens. Further, we demonstrate that B-intrinsic TLR9 deletion results in increased systemic inflammation and immune-complex (IC) glomerulonephritis despite intact TLR signaling within the myeloid compartment. These data stress the critical importance of dysregulated B cell-intrinsic TLR signaling in the pathogenesis of SLE.

INTRODUCTION

Despite numerous potential autoantigen targets, patients with SLE frequently develop a restricted autoantibody repertoire targeting nucleic acid-associated antigens. In addition to exogenous pathogens, the Toll-like receptor (TLR) family of germ-line encoded, pattern-recognition receptors are able to recognize endogenous ligands. Nucleic acid-containing apoptotic particles promote activation of autoreactive B cells via dual B cell receptor (BCR)/Toll-like receptor (TLR)-mediated signals, thereby explaining the prominence of antinuclear Abs in autoimmunity (1–3). The Myd88-dependent, endosomal receptors TLR7 and TLR9 are critical in this context, with TLR7 required for the generation of Abs targeting RNA and RNA-associated proteins, while TLR9 activation promotes production of Abs targeting dsDNA and chromatin (4–7).

Importantly, two alternate, but not mutually-exclusive, mechanisms may explain the role of TLR7 and TLR9 in autoimmune pathogenesis *in vivo*. Dual BCR/TLR activation may either promote a B cell-intrinsic break in tolerance, or IC-mediated TLR activation of plasmacytoid dendritic cells may promote autoimmunity via increased type 1 IFN production (4, 8). In addition, *tlr7*-deficient lupus-prone mice are significantly protected from autoimmunity, whereas disease is exacerbated in *tlr9*$^{-/-}$ autoimmune strains (1–3). The mechanisms underlying accelerated autoimmunity in the absence of TLR9 remain unclear. However, *tlr9*$^{-/-}$ MRL.Mp$^{lpr/lpr}$ mice develop greater plasmacytoid dendritic cell activation and increased serum IFN-α levels suggesting that loss of *tlr9* in the myeloid compartment exacerbates autoimmunity on the MRL.Mp$^{lpr/lpr}$ background (6).

While several models (9–13) have implicated B cell Myd88 signaling in autoimmune pathogenesis, the B-intrinsic impact of TLR7 and TLR9 has only been addressed in a limited number of studies. The role of B cell-intrinsic TLR7 signaling was evaluated in two studies using the TLR7 transgenic (*tlr7Tg*) model of spontaneous autoimmunity. First, using a chimeric transplant strategy comparing wild-type (WT) vs TLR7 transgenic (*tlr7Tg*) hematopoietic cells, *Walsh et al.* demonstrated that *tlr7Tg* B cells are preferentially recruited into germinal centers (GC) and generate CD138^{+} plasmablasts (14). Second, *Hwang et al.* used a CD19^{Cre} recombinase system to normalize B cell TLR7 expression in a low copy *tlr7Tg* strain crossed with the *Sle1* lupus susceptibility locus. B cell-intrinsic TLR7 normalization decreased RNA-associated anti-SnRNP titers, but did not impact GC and plasma cell formation and only moderately reduced autoimmune glomerulonephritis (15). To address the B cell-intrinsic impact of TLR9, a recent study utilized MRL.*Fas*^{lpr} mixed bone marrow (BM) chimeras in which *tlr9*-deficiency was primarily limited to the B cell compartment and demonstrated a specific reduction in anti-nucleosome reactivity. Whether B cell-intrinsic *tlr9* deletion accelerated systemic autoimmunity, however, was not addressed in that study (16).

We recently developed a murine model of autoimmunity that provides important information regarding how self-reactive B cells are initially activated and can drive generation of pathogenic Ab (12). In this model, B cells, but not other hematopoietic lineages, harbor a mutation that abolishes the expression of Wiskott Aldrich syndrome protein (WASp). In the absence of WASp, peripheral B cells are rendered mildly hyper-

responsive to both B cell receptor (BCR) and Toll-like receptor (TLR) ligands. In this setting, Wiskott-Aldrich syndrome (WAS)-null ($was^{-/-}$) B cells drive the development of humoral autoimmunity that is characterized by spontaneous GCs, class-switched IgG2c autoantibodies and IC glomerulonephritis. Disease development is dependent on wild-type $CD4^+$ T cells and MyD88-dependant B cell-intrinsic TLR signaling. An important advantage of the WASp chimera model is that dysregulated immune responses are limited to the B cell compartment, allowing genetic manipulation in a B cell-intrinsic fashion. In the current study, we detail the relative contributions of B cell TLR signaling in humoral autoimmunity and demonstrate that B cell-intrinsic TLR7 vs TLR9 activation is sufficient to alter the autoantibody repertoire. In addition, we demonstrate that B cell TLR7 and TLR9 signals exert opposing pathogenic and protective effects on systemic inflammation and autoimmune pathology.

MATERIALS AND METHODS

Mice

Ly.5.1$^+$ and Ly5.2$^+$ C57BL/6, *μMT*, *was*$^{-/-}$, *tlr7*$^{-/-}$ and *tlr9*$^{-/-}$ mice were bred and maintained in the specific pathogen-free (SPF) animal facility of Seattle Children's Research Institute (Seattle, WA). All animal studies were conducted in accordance with Seattle Children's Research Institute IACUC approved protocols.

Bone Marrow Transplantation

WT, *was*$^{-/-}$, *was*$^{-/-}$.*tlr7*$^{-/-}$ or *was*$^{-/-}$.*tlr9*$^{-/-}$ donor BM and μMT BM (20:80 ratio, 5×10^6 total BM), was injected into lethally irradiated (450cGy x 2 doses) μMT recipients. Chimeras were sacrificed at 24–36 weeks post-transplant. For CD4-depletion assays, mice were treated weekly with IP injection of 250μg anti-CD4 (GK1.5) or isotype control (rat IgG2b) Ab (UCSF Antibody Core) from 5–24 weeks post-transplant, as described (12). Data are representative of four (B^{WT}, B$^{WAS-/-}$, and B$^{W/TLR9-/-}$), three (B$^{W/TLR7-/-}$) or two (B$^{WAS-/-}$ CD4 depletion) independent experimental cohorts.

Flow Cytometry and Antibodies

Flow cytometry was performed as described (12). Antibodies used: B220 (RA3-6B2), CD4 (RM4-5), Thy1.2 (53-2.1), CD138 (281-2), CXCR5 (2G8) from BD Biosciences; CD62L (MEL-14), CD11c (N418), Gr-1 (RB6-8C5), Ly5.1 (A20), Ly5.2 (104), CD11b (M1/70), GL7 (GL-7), PD-1 (J43) from eBioscience; goat anti-mouse IgM-, IgG-, IgG2c- HRP conjugated, unlabeled, or isotype from Southern Biotechnology; CD19 (ID3), CD44 (IM7) from BioLegend; PNA (Fl-1071) from Vector Labs; and Fas (Jo2) from BD Pharmingen.

Measurement of autoantibodies

For ANA assays and determination of dsDNA reactivity by kinetoplast staining, diluted serum (1:200 for ANA or 1:50 for kinetoplast) was added to fixed Hep-2 ANA slides (Bio-Rad 30472) or *Crithidia luciliae* slides (Bio-Rad 31069). FITC-conjugated goat anti-mouse IgG served as the detection antibody and slides were counterstained with DAPI. Fluorescence images were obtained using Leica DM6000B microscope, Leica DFL300 FX camera, and Leica Application Suite Advanced Fluorescence software at 40x with a constant

5 second (ANA) or 2 second (kinetoplast) exposure. ANAs were scored as nuclear homogeneous, nucleolar, cytoplasmic or a combination of these patterns. Kinetoplast reactivity was defined by co-localization of DAPI-positive *C. luciliae* DNA and IgG FITC staining; with staining intensity scored from 0–3. ANA patterns and kinetoplast intensity were scored by two independent observers blinded to genotype.

For specific Ab ELISAs, 96 well Immuno plates (Nunc) were coated with: calf thymus dsDNA (100ug/ml; Sigma-Aldrich D3664-5X2MG); sm/RNP (5ug/ml; Arotec Diagnostic Limited ATR01-10); PC-BSA (10ug/ml; Biosearch Technologies PC-1011-10); or MDA-LDL (10ug/ml; Academy Bio-medical Co. 20P-MD-L110). Plates were blocked for 1 hour with 1% BSA/PBS prior to addition of diluted serum for 2 hours. Specific Ab were detected using goat anti-mouse IgM-, IgG- or IgG2c-HRP (1:2000 dilution; Southern Biotechnology Associates) and peroxidase reactions developed using OptEIA TMB substrate (BD Biosciences). Absorbance at 450nm was read using a Victor 3 plate reader (PerkinElmer) and data analyzed using GraphPad Prism (GraphPad Software, Inc.). Autoantigen microarrays were performed at the UT Southwestern Medical Center Microarry Core Facility, Dallas, TX (17).

Spleen and kidney immunofluorescence staining

Mouse spleens and kidneys were embedded in OCT compound and snap frozen over liquid nitrogen. 10 μm sections were cut on a cryostat, mounted on Superfrost plus slides, and fixed in −20°C acetone for 20 minutes. After rehydration in staining buffer (PBS, 1% goat serum, 1% BSA, 0.1% Tween-20), slides were stained with: B220-PE, CD4-FITC and GL7-APC (spleen); or, IgG-FITC, IgG2c-FITC, or C3-FITC (kidney). Images were acquired using a Leica DM6000B microscope, Leica DFL300 FX camera, and Leica Application Suite Advanced Fluorescence software. For glomerular immune-complex quantification, images were obtained using a constant exposure and scored from 0–3 by two independent observers blinded to genotype.

Histopathology

Tissues were fixed in 10% neutral buffered formalin, embedded in paraffin and tissues sections stained with Hematoxylin and eosin (H&E) (lung, liver, pancreas) or Jones' methenamine silver-Periodic acid-Schiff (kidney) according to standard practices. Immunohistochemistry staining was performed using a Leica Bond–automated immunostainer and HRP-conjugated secondary Abs. Histology images were acquired using a Nikon OptiPhot-2 microscope and a Canon Eos 5D Mark II camera. Tissue sections were examined by a board-certified veterinary pathologist (D.L.) who was blinded to study design. Kidney sections were analyzed by two observers blinded to genotype (K.L.H. and C.E.A.) and scored from 0–2 based on degree of mesangial expansion, GBM thickening/reduplication and glomerular hypercellularity. For quantification of MAC-2 area, glomeruli were manually delineated in 4 independent kidney sections and MAC-2^{+} area as a percentage of glomerular area determined using Image Pro Plus (Media Cybernetics, Inc. Rockville, MD).

Statistical Evaluation

P-values were calculated using one-way ANOVA, followed by Tukey's multiple comparison test (GraphPad Software, Inc.).

RESULTS

B cell-intrinsic TLR7 and TLR9 signals alter the autoantibody repertoire

To test the impact of B cell-intrinsic TLR7 and TLR9 deletion in humoral autoimmunity, we generated mixed bone marrow (BM) chimeras by transplanting a mix of 20% WT, Wiskott-Aldrich syndrome (WAS)-null (*was*$^{-/-}$), double-deficient *was*$^{-/-}$.*tlr7*$^{-/-}$, or *was*$^{-/-}$.*tlr9*$^{-/-}$ BM with 80% B cell-deficient μMT BM into lethally irradiated (450cGy x 2 doses) μMT recipients. After reconstitution, all B cells were donor-derived (either WT, *was*$^{-/-}$, *was*$^{-/-}$.*tlr7*$^{-/-}$, or *was*$^{-/-}$.*tlr9*$^{-/-}$), while ~80% of myeloid cells and >97% CD4$^+$ T cells were wild-type (not shown). Utilizing this strategy, in the TLR-deficient cohorts, all B cells, but only ~20% of myeloid cells, lacked TLR7 or TLR9. Respective B cell chimeras will henceforth be referred to as B^{WT}, B$^{WAS-/-}$, B$^{W/TLR7-/-}$ and B$^{W/TLR9-/-}$.

We initially screened for autoimmunity using fluorescent antinuclear antibody (ANA) assays. The majority of B$^{WAS-/-}$ were ANA positive with mixed homogenous and nucleolar staining patterns, consistent with both DNA and RNA Ab reactivity. In contrast, B$^{W/TLR7-/-}$ ANA staining was homogenous with no nucleolar reactivity, while B$^{W/TLR9-/-}$ showed nucleolar and cytoplasmic, but not homogenous, ANA reactivity (Fig. 1A). These altered ANA staining patterns suggested a B-intrinsic impact of TLR7 vs. TLR9 on RNA- and DNA-associated Abs, which we evaluated using specific autoantigen ELISAs. Prior reports have demonstrated persistent anti-dsDNA Ab in *tlr9*-deficient murine lupus models; an effect attributed to a lack of DNA specificity of standard anti-dsDNA ELISA assays (6, 18). Although we noted anti-dsDNA Ab by ELISA in B$^{W/TLR9-/-}$, DNA-reactivity by highly-specific *Crithidia luciliae* kinetoplast staining was abrogated in B$^{W/TLR9-/-}$, but unaffected in B$^{W/TLR7-/-}$ (Fig. 1B, Supplemental Fig. 1A). In contrast, RNA-associated anti-sm/RNP Ab were abolished in B$^{W/TLR7-/-}$. Further, anti-sm/RNP Ab titers of the pathogenic IgG2c subclass were significantly increased in B$^{W/TLR9-/-}$ vs. B$^{WAS-/-}$ chimeras, an observation consistent with elevated anti-RNA titers in *tlr9*$^{-/-}$ MRL.Mp$^{lpr/lpr}$ mice (Fig. 1C). Therefore, the requirement for TLR7 in anti-RNA and TLR9 in anti-DNA Ab production is B cell-intrinsic; and lack of TLR9 enhances anti-RNA Ab formation in a B-intrinsic manner.

Generation of Ab targeting non-nuclear antigens was recently shown to be Myd88 dependent (11, 19), but the specific TLRs responsible for these Ab specificities have not been determined. For this reason, we measured IgG reactivity to apoptotic cell epitopes malondialdehyde conjugated with low-density lipoprotein (MDA-LDL) and phosphoryl choline (PC). In contrast to abrogation of anti-RNA responses, anti-apoptotic IgG responses were decreased in B$^{W/TLR7-/-}$; but were not absent. Rather, we noted a specific decrease in pathogenic IgG2c subclass titers. Since we previously observed a lack of anti-dsDNA IgG2c in the absence of cognate T cell help (12), we measured anti-PC and anti-MDA-LDL IgG2c subclass titers in B$^{WAS-/-}$ treated weekly with monoclonal CD4-depleting antibody. In the absence of CD4$^+$ T cells, B$^{WAS-/-}$ chimeras developed markedly reduced IgG2c Ab

targeting PC and MDA-LDL; findings that mirrored B$^{W/TLR7-/-}$ (Fig. 2A, 2B). Therefore, in addition to the B cell-intrinsic requirement for TLR7 in generating Abs targeting RNA and RNA-associated antigens (Fig. 1C, and (15)), our data demonstrate that B cell-intrinsic TLR7 signals are required for generation of class-switched Abs targeting non-nuclear, apoptotic antigens.

Finally, to quantify the impact of B cell *tlr7* vs. *tlr9* deficiency on the diversity of the autoantibody repertoire of B$^{WAS-/-}$ chimeras, sera was evaluated for reactivity to 88 distinct autoantigens by microarray. While B$^{W/TLR7-/-}$ demonstrated a broad reduction in serum Ab titers, the reactivity of B$^{W/TLR9-/-}$ sera was *increased* relative to B$^{WAS-/-}$ to a wide-range of different autoantigens (Fig. 2C). Consistent with our ELISA data, these Abs were predominantly of the pathogenic IgG2c subclass (Supplemental Fig. 1B). While absolutely required for the generation of anti-dsDNA Abs, TLR9 thus acts B-intrinsically to limit Ab responses to RNA-associated autoantigens, apoptotic cell epitopes and a broad range of disease-associated autoantigens.

B cell-intrinsic TLR7 and TLR9 exert opposing signals on immune activation

We previously demonstrated that B$^{WAS-/-}$ chimeras develop systemic inflammation that is dependent on B cell Myd88 signaling (12). B cell TLR7 and TLR9 signaling exerted opposing impacts on immune activation in this model, as splenic inflammation is exacerbated in B$^{W/TLR9-/-}$, but abrogated in B$^{W/TLR7-/-}$. Relative to B$^{WAS-/-}$, B$^{W/TLR9-/-}$ chimeras developed increased splenomegaly, without marked alterations in total B cell numbers (Fig. 3A, 3B). Notably, splenomegaly in B$^{WAS-/-}$ and B$^{W/TLR9-/-}$ resulted from a significant expansion of CD4$^+$ T cells, CD11b$^+$GR1^{LO} monocyte/macrophages and CD11b$^+$GR1$^+$ neutrophils. Consistent with a role for TLR9 in limiting autoimmune responses, B cell-intrinsic TLR9 deletion resulted in statistically greater numbers of CD4$^+$ T cells and monocyte/macrophages relative to B$^{WAS-/-}$, with a trend towards more neutrophils (Fig. 3C, 3D).

Although total B cell numbers were similar, activated B cell subsets including PNA$^+$FAS$^+$GL7$^+$ GC B cells and B220^{LO}CD138$^+$ plasma cells/plasmablasts were markedly expanded in spleens of B$^{WAS-/-}$ and B$^{W/TLR9-/-}$ chimeras (Fig. 4A, 4C). In addition, splenic immunofluorescence staining revealed spontaneous GL7$^+$ GCs in B$^{WAS-/-}$ and B$^{W/TLR9-/-}$ mice, which were absent in B$^{W/TLR7-/-}$ (Fig. 4D). Relative to B$^{WAS-/-}$, B$^{W/TLR9-/-}$ animals exhibited a higher percentage of GC B cells with greater numbers of splenic CD138$^+$ plasma cells/plasmablasts, suggesting that B cell-intrinsic TLR9 signals serve to limit B cell activation. Consistent with this, total serum IgM, IgG and IgG2c Ab titers were markedly elevated in B$^{W/TLR9-/-}$ mice relative to B$^{W/TLR7-/-}$ mice, with a trend towards greater Ab titers than B$^{WAS-/-}$ chimeras (Fig 4E).

B$^{WAS-/-}$ and B$^{W/TLR9-/-}$ also developed significant expansion of autoimmune disease-associated CD11b$^+$CD11c$^+$ "age-associated B cells" (ABCs), with up to 75% of total B cells expressing CD11b and CD11c in B$^{W/TLR9-/-}$, exceeding the percentage ABCs previously reported in aged NZB/WF1 and *Mer*$^{-/-}$ autoimmune strains (20, 21). In keeping with importance of chronic TLR7 activation in ABC generation, this population was absent B$^{W/TLR7-/-}$ (Fig. 4B).

In addition to B cell activation, CD4$^+$ effector/memory (EM) subsets (CD44^{HI}CD62L^{LO} and CD44^{HI}CD62L^{HI}) were increased in B$^{WAS-/-}$ and B$^{W/TLR9-/-}$ (with relatively greater T cell activation in B$^{W/TLR9-/-}$), while the number of CD44^{LO}CD62L^{HI} naïve CD4 T cells did not differ between experimental groups (Fig. 5A). Consistent with greater GC B cell numbers, PD1$^+$CXCR5$^+$ T follicular helper cells were also expanded in B$^{WAS-/-}$ and B$^{W/TLR9-/-}$ (Fig. 5B). B cell-intrinsic TLR7 activation appears critical for T cell activation in this model, as CD4$^+$ effector/memory (EM) and T follicular helper cell subset expansion is abrogated in B$^{W/TLR7-/-}$.

In conclusion, B cell-intrinsic activation of autoreactive *was*$^{-/-}$ B cells via TLR7 promotes global immune activation and expansion of activated B and T cell populations; while B cell TLR9 signaling serves to limit these processes.

B cell intrinsic TLR7 signaling promotes systemic autoimmunity

Aged B$^{WAS-/-}$ and B$^{W/TLR9-/-}$ chimeras demonstrated diffuse inflammation and lymphoid infiltrates involving multiple organs, in particular the lungs and liver; findings that were absent in all B^{WT} and B$^{W/TLR7-/-}$ animals evaluated (Fig. 6A). Immunohistochemistry staining demonstrated that these lymphoid infiltrates were consistent with ectopic lymphoid follicles comprising separate B220$^+$ B cell and CD3$^+$ T cells zones (Fig. 6B). The presence of ectopic lymphoid tissues within target organs has been reported in several human autoimmune diseases, including rheumatoid arthritis and type 1 diabetes, and is correlated with disease severity in autoimmunity (22). We demonstrate that hyper-responsive *was*$^{-/-}$ B cells are sufficient to recruit WT T cells to ectopic lymphoid follicles in a TLR7-dependent manner, reinforcing the critical role of B cell-intrinsic TLR7 signals in the pathogenesis of systemic autoimmunity.

B cell TLR7 deletion eliminates, while TLR9 loss exacerbates, IC glomerulonephritis

Given divergent impacts on Ab production and systemic inflammation, we evaluated the role of B cell-intrinsic TLR signaling on autoimmune glomerulonephritis. B$^{WAS-/-}$ chimeras develop inflammatory glomerulonephritis characterized by deposition of class-switched Ab, activated complement and recruitment of MAC-2$^+$ macrophages (12). In keeping with an overall decrease in Ab titer and systemic inflammation, B$^{W/TLR7-/-}$ chimeras did not develop glomerulonephritis (Fig. 7A), an observation consistent with decreased glomerulonephritis in *tlr7*$^{-/-}$ MRL/Mp$^{lpr/lpr}$ mice (6). Despite absent histologic glomerulonephritis, evaluation of glomerular Ig deposition by immunofluorescence staining showed persistent glomerular IgG in B$^{W/TLR7-/-}$ chimeras (albeit at lower levels than B$^{WAS-/-}$ and B$^{W/TLR9-/-}$) (Fig. 7B). However, deposition of the pathogenic IgG2c subclass was absent in B$^{W/TLR7-/-}$ (Fig. 7C). In keeping with the role for IgG2c in complement and Fc-receptor activation (23), C3 complement deposition was absent in B$^{W/TLR7-/-}$ and glomerular MAC-2$^+$ macrophages were not increased over B^{WT} controls (Fig. 7D,E).

In contrast to the protective effect of B cell TLR7 deletion, B$^{WAS-/-}$ and B$^{W/TLR9-/-}$ chimeras developed significant glomerulonephritis characterized by mesangial expansion, glomerular basement membrane thickening and glomerular hypercellularity (Fig. 7A). In keeping with increased serum IgG2c Ab, B$^{W/TLR9-/-}$ mice demonstrated statistically greater

glomerular IgG2c deposition than $B^{WAS-/-}$, with a trend towards greater C3 complement deposition and abundant infiltration by MAC-2$^+$ macrophages, likely recruited by glomerular IgG2c ICs binding activating Fc-receptors (Fig. 7B-E). Increased IC glomerulonephritis in $B^{W/TLR9-/-}$ parallels accelerated autoimmune pathology in *tlr9$^{-/-}$* MRL/Mp$^{lpr/lpr}$ mice, but demonstrates that the disease exacerbating effects of TLR9 deletion can occur independently of the lack of TLR9 expression in the majority of the myeloid compartment.

DISCUSSION

The importance of the Myd88-dependant toll-like receptors TLR7 and TLR9 in lupus pathogenesis has been clearly established (1–3). In this context, global deletion of TLR7 in murine lupus models protects against autoimmunity, while TLR9 deficiency paradoxically exacerbates disease (4–7). The mechanisms underlying these divergent effects of TLR7 and TLR9 remain unclear, in part because studies involving globally gene deficient autoimmune strains are unable to address the differential impacts of TLR signaling on B cells vs. type 1 IFN-producing plasmacytoid dendritic cells. Our study provides the novel observation that B cell-intrinsic deletion of TLR7 or TLR9 recapitulates several of the key features of global TLR7/TLR9 deficiency in murine lupus models, despite intact TLR signaling within the myeloid compartment.

In this context, our data provide several important new insights into autoimmune pathogenesis. First, this study is the first to compare the B cell-intrinsic impact of TLR7 vs. TLR9 in parallel models of murine autoimmunity. Similar to global TLR7/TLR9 deletion in murine lupus models, we demonstrate that B cell-intrinsic TLR7 and TLR9 signals are required for *in vivo* generation of RNA- and DNA-reactive Ab, respectively. In addition, we also establish TLR7 as the major Myd88-dependent receptor responsible for B intrinsic breaks in tolerance to a broad range of non-nuclear, tissue-specific autoantigens.

Second, we identify a critical role for B cell-intrinsic TLR7 signals in sustaining spontaneous autoimmune GC responses. While the absence of anti-sm/RNP antibodies in $B^{W/TLR7-/-}$ may have been predicted from *in vitro* studies (24), the observation that antibodies targeting apoptotic and phospholipid epitopes develop in $B^{W/TLR7-/-}$, but fail to undergo efficient CSR suggests an additional role for B cell TLR7 signaling in enhancing GC responses during autoimmune disease; a finding that parallels the requirement for TLR7 in Ab responses to chronic viral infection (25).

Third, we document a striking expansion of effector and T$_{FH}$ CD4$^+$ T cells in $B^{WAS-/-}$ and $B^{W/TLR9-/-}$ animals. Similar expansion of the effector/memory T cell compartment has been documented on the lupus-prone MRL/Mp$^{lpr/lpr}$ background (6), although it should be noted that CD4$^+$ T cells in our model are genetically WT and not Fas-deficient. Our data, therefore, suggests that BCR/TLR-mediated activation of autoreactive B cells directly promotes T cell proliferation and activation during autoimmunity. These data are consistent with recent reports describing decreased T effector/memory expansion in the setting of B cell-intrinsic Myd88 deletion in the MRL.*Fas*^{lpr} and Lyn deficient models of autoimmunity (11, 13). Our data suggests that B cell TLR7 is likely the major Myd88-dependent receptor

driving this CD4^{+} T cell activation. Surprisingly, dual BCR/TLR7 B cell activation was also sufficient for the establishment of ectopic lymphoid follicles within target organs, as have previously been described in several human autoimmune diseases (22). Although not formally demonstrated, we predict that these expanded effector/memory T cell compartments are enriched for autoreactive T cell clones, supporting the emerging hypothesis that activated autoreactive B cells can initiate breaks in T cell tolerance.

Forth, we demonstrate the importance of autoantibody isotype (in particular IgG2a/c) in promoting autoimmune nephritis. Despite producing anti-dsDNA Ab, B$^{W/TLR7-/-}$ fail to develop IC glomerulonephritis. These renal protective effects of TLR7 deletion despite persistent DNA-reactive Ab are surprising given clinical data implicating anti-dsDNA Abs in lupus nephritis (26). In keeping with this paradox, we observed glomerular IgG deposition by immunofluorescence in B$^{W/TLR7-/-}$, in the absence of histologic glomerulonephritis. However, deposition of the pathogenic Ig subclass IgG2c was abrogated in the absence of B cell TLR7. In keeping with the role for IgG2c in promoting complement activation and activation of myeloid Fc-receptors (23), glomerular C3 deposition and recruitment of inflammatory macrophages was absent in B$^{W/TLR7-/-}$. These data emphasize the need to consider IgG subclass in addition to Ab specificity in mediating end-organ damage in SLE

Finally, we show that B cell-intrinsic TLR9 deletion: enhances class-switched Abs targeting RNA-associated antigens and broadens the autoantibody repertoire; exacerbates systemic inflammation and expansion of activated CD4^{+} T cell and myeloid populations; and promotes glomerular deposition of pathogenic IgG2c IC. Although protective roles for TLR9 in autoimmunity have been described in several murine autoimmune models, how TLR9 deletion promotes autoimmunity has not yet been determined. Potential underlying mechanisms include: enhanced interaction of TLR7 with the shared endoplasmic reticulum trafficking protein Unc93b1 in the setting of TLR9-deletion (27); facilitation of entry of autoreactive cells into the mature B cell repertoire (16); or decreased generation of TLR9-dependent regulatory B cells (2). Our study makes the important observation that B cell-intrinsic TLR9 deletion can accelerate autoimmunity despite largely intact myeloid TLR signaling.

Importantly, however, our data does not exclude the possibility that myeloid TLR7 and TLR9 signals may exert additional impacts on lupus pathogenesis. Two recent studies, utilizing a cre-recombinase strategy to delete the TLR adaptor Myd88 in CD11c^{+} dendritic cells, demonstrated that myeloid TLR activation accelerates autoimmunity, likely via enhanced type 1 IFN production by IC-mediated activation of plasmacytoid dendritic cells (11, 13). Given this observation, it will be important to evaluate whether deletion of myeloid TLR7 vs. TLR9 exerts similar divergent effects on autoimmune pathogenesis. In this regard, a potential caveat of our study is that reconstitution with an 80:20 ratio of μMT:donor (*was*$^{-/-}$, *was*$^{-/-}$.*tlr7*$^{-/-}$, or *was*$^{-/-}$.*tlr9*$^{-/-}$) BM, will result in ~20% myeloid cells also lacking TLR7 or TLR9. However, since the majority of myeloid cells (~80%) in our model are TLR sufficient, it is highly likely that our data reflect the B cell-intrinsic effects of TLR7 vs TLR9 in autoimmune pathogenesis.

In conclusion, our study provides critical new insights into how dual BCR and TLR signals promote B cell activation resulting in class-switched antibody production, CD4^{+} T cell activation and the development of IC glomerulonephritis. B cell TLR7 and TLR9 exert opposing impacts in this process, reinforcing the importance of dysregulated B cell TLR signaling in autoimmunity and informing efforts to therapeutically target TLR signals in SLE and other disorders characterized by autoantibody production.

Supplementary Material

Refer to Web version on PubMed Central for supplementary material.

Abbreviations used

ABC	age-associated B cells
ANA	antinuclear antibody
BM	bone marrow
CSR	class switch recombination
EM	effector/memory T cells
GC	germinal center
IC	immune complex
MDA-LDL	malondialdehyde conjugated with low-density lipoprotein
PC	phosphoryl choline
SLE	systemic lupus erythematosus
TFH	T follicular helper cells
μMT	B cell-deficient
WAS	Wiskott-Aldrich syndrome
WASp	Wiskott-Aldrich syndrome protein

References

1. Shlomchik MJ. Activating systemic autoimmunity: B's, T's, and tolls. Curr Opin Immunol. 2009; 21:626–633. [PubMed: 19800208]

2. Green NM, Marshak-Rothstein A. Toll-like receptor driven B cell activation in the induction of systemic autoimmunity. Semin Immunol. 2011; 23:106–112. [PubMed: 21306913]

3. Rawlings DJ, Schwartz MA, Jackson SW, Meyer-Bahlburg A. Integration of B cell responses through Toll-like receptors and antigen receptors. Nat Rev Immunol. 2012; 12:282–294. [PubMed: 22421786]

4. Christensen SR, Kashgarian M, Alexopoulou L, Flavell RA, Akira S, Shlomchik MJ. Toll-like receptor 9 controls anti-DNA autoantibody production in murine lupus. J Exp Med. 2005; 202:321–331. [PubMed: 16027240]

5. Berland R, Fernandez L, Kari E, Han JH, Lomakin I, Akira S, Wortis HH, Kearney JF, Ucci AA, Imanishi-Kari T. Toll-like receptor 7-dependent loss of B cell tolerance in pathogenic autoantibody knockin mice. Immunity. 2006; 25:429–440. [PubMed: 16973388]

6. Christensen SR, Shupe J, Nickerson K, Kashgarian M, Flavell RA, Shlomchik MJ. Toll-like receptor 7 and TLR9 dictate autoantibody specificity and have opposing inflammatory and regulatory roles in a murine model of lupus. Immunity. 2006; 25:417–428. [PubMed: 16973389]

7. Lartigue A, Courville P, Auquit I, Francois A, Arnoult C, Tron F, Gilbert D, Musette P. Role of TLR9 in anti-nucleosome and anti-DNA antibody production in lpr mutation-induced murine lupus. J Immunol. 2006; 177:1349–1354. [PubMed: 16818796]

8. Yasuda K, Richez C, Maciaszek JW, Agrawal N, Akira S, Marshak-Rothstein A, Rifkin IR. Murine dendritic cell type I IFN production induced by human IgG-RNA immune complexes is IFN regulatory factor (IRF)5 and IRF7 dependent and is required for IL-6 production. J Immunol. 2007; 178:6876–6885. [PubMed: 17513736]

9. Groom JR, Fletcher CA, Walters SN, Grey ST, Watt SV, Sweet MJ, Smyth MJ, Mackay CR, Mackay F. BAFF and MyD88 signals promote a lupuslike disease independent of T cells. J Exp Med. 2007; 204:1959–1971. [PubMed: 17664289]

10. Ehlers M, Fukuyama H, McGaha TL, Aderem A, Ravetch JV. TLR9/MyD88 signaling is required for class switching to pathogenic IgG2a and 2b autoantibodies in SLE. J Exp Med. 2006; 203:553–561. [PubMed: 16492804]

11. Teichmann LL, Schenten D, Medzhitov R, Kashgarian M, Shlomchik MJ. Signals via the adaptor MyD88 in B cells and DCs make distinct and synergistic contributions to immune activation and tissue damage in lupus. Immunity. 2013; 38:528–540. [PubMed: 23499488]

12. Becker-Herman S, Meyer-Bahlburg A, Schwartz MA, Jackson SW, Hudkins KL, Liu C, Sather BD, Khim S, Liggitt D, Song W, Silverman GJ, Alpers CE, Rawlings DJ. WASp-deficient B cells play a critical, cell-intrinsic role in triggering autoimmunity. J Exp Med. 2011; 208:2033–2042. [PubMed: 21875954]

13. Hua Z, Gross AJ, Lamagna C, Ramos-Hernandez N, Scapini P, Ji M, Shao H, Lowell CA, Hou B, Defranco AL. Requirement for MyD88 Signaling in B Cells and Dendritic Cells for Germinal Center Anti-Nuclear Antibody Production in Lyn-Deficient Mice. J Immunol. 2013

14. Walsh ER, Pisitkun P, Voynova E, Deane JA, Scott BL, Caspi RR, Bolland S. Dual signaling by innate and adaptive immune receptors is required for TLR7-induced B-cell-mediated autoimmunity. Proc Natl Acad Sci U S A. 2012; 109:16276–16281. [PubMed: 22988104]

15. Hwang SH, Lee H, Yamamoto M, Jones LA, Dayalan J, Hopkins R, Zhou XJ, Yarovinsky F, Connolly JE, Curotto de Lafaille MA, Wakeland EK, Fairhurst AM. B cell TLR7 expression drives anti-RNA autoantibody production and exacerbates disease in systemic lupus erythematosus-prone mice. J Immunol. 2012; 189:5786–5796. [PubMed: 23150717]

16. Nickerson KM, Christensen SR, Cullen JL, Meng W, Luning Prak ET, Shlomchik MJ. TLR9 promotes tolerance by restricting survival of anergic anti-DNA B cells, yet is also required for their activation. J Immunol. 2013; 190:1447–1456. [PubMed: 23296704]

17. Li QZ, Zhou J, Wandstrat AE, Carr-Johnson F, Branch V, Karp DR, Mohan C, Wakeland EK, Olsen NJ. Protein array autoantibody profiles for insights into systemic lupus erythematosus and incomplete lupus syndromes. Clin Exp Immunol. 2007; 147:60–70. [PubMed: 17177964]

18. Isenberg DA, Dudeney C, Williams W, Addison I, Charles S, Clarke J, Todd-Pokropek A. Measurement of anti-DNA antibodies: a reappraisal using five different methods. Ann Rheum Dis. 1987; 46:448–456. [PubMed: 3498446]

19. Koh YT, Scatizzi JC, Gahan JD, Lawson BR, Baccala R, Pollard KM, Beutler BA, Theofilopoulos AN, Kono DH. Role of nucleic acid-sensing TLRs in diverse autoantibody specificities and anti-nuclear antibody-producing B cells. J Immunol. 2013; 190:4982–4990. [PubMed: 23589617]

20. Rubtsov AV, Rubtsova K, Fischer A, Meehan RT, Gillis JZ, Kappler JW, Marrack P. Toll-like receptor 7 (TLR7)-driven accumulation of a novel CD11c(+) B-cell population is important for the development of autoimmunity. Blood. 2011; 118:1305–1315. [PubMed: 21543762]

21. Hao Y, O'Neill P, Naradikian MS, Scholz JL, Cancro MP. A B-cell subset uniquely responsive to innate stimuli accumulates in aged mice. Blood. 2011; 118:1294–1304. [PubMed: 21562046]

22. Carragher DM, Rangel-Moreno J, Randall TD. Ectopic lymphoid tissues and local immunity. Semin Immunol. 2008; 20:26–42. [PubMed: 18243731]

23. Nimmerjahn F, Ravetch JV. Divergent immunoglobulin g subclass activity through selective Fc receptor binding. Science. 2005; 310:1510–1512. [PubMed: 16322460]

24. Lau CM, Broughton C, Tabor AS, Akira S, Flavell RA, Mamula MJ, Christensen SR, Shlomchik MJ, Viglianti GA, Rifkin IR, Marshak-Rothstein A. RNA-associated autoantigens activate B cells by combined B cell antigen receptor/Toll-like receptor 7 engagement. J Exp Med. 2005; 202:1171–1177. [PubMed: 16260486]

25. Clingan JM, Matloubian M. B Cell-Intrinsic TLR7 Signaling Is Required for Optimal B Cell Responses during Chronic Viral Infection. J Immunol. 2013

26. Isenberg DA, Manson JJ, Ehrenstein MR, Rahman A. Fifty years of anti-ds DNA antibodies: are we approaching journey's end? Rheumatology (Oxford). 2007; 46:1052–1056. [PubMed: 17500073]

27. Fukui R, Saitoh S, Kanno A, Onji M, Shibata T, Ito A, Onji M, Matsumoto M, Akira S, Yoshida N, Miyake K. Unc93B1 restricts systemic lethal inflammation by orchestrating Toll-like receptor 7 and 9 trafficking. Immunity. 2011; 35:69–81. [PubMed: 21683627]
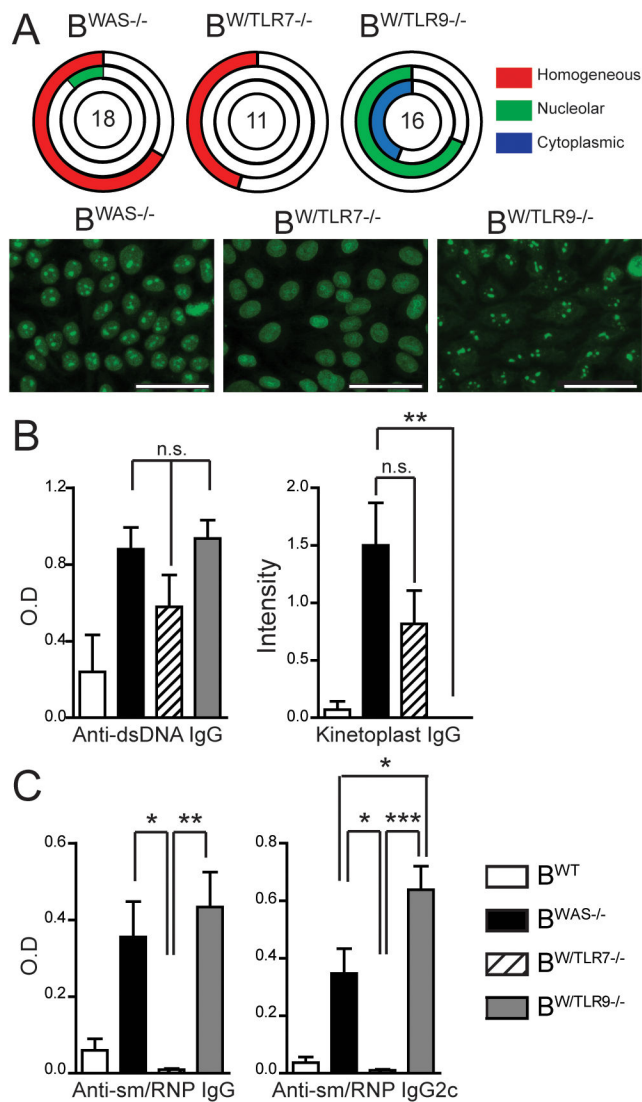
Figure 1. B cell-intrinsic TLR7 and TLR9 signals promote anti-nuclear Ab production

(A) Upper: ANA staining patterns were scored as homogeneous, nucleolar, or cytoplasmic by two independent, blinded observers. Unfilled portion of circle represents ANA-negative animals. The number in the circle represents the total number of mice analyzed. Lower: Representative ANA images showing: combined homogeneous/nucleolar staining in $B^{WAS-/-}$; homogenous pattern with nucleolar sparing in $B^{W/TLR7-/-}$; nucleolar and cytoplasmic staining in $B^{W/TLR9-/-}$. Bars, 50μm. (B) Anti-dsDNA IgG Ab by ELISA and kinetoplast staining. (C) Anti-sm/RNP IgG and IgG2c Ab by ELISA. (B, C) Mean ± s.e.m. *, $P<0.05$; **, $P<0.01$; ***, $P<0.001$. (A–C) Total mice analyzed: B^{WT} (n=6), $B^{WAS-/-}$ (n=18) $B^{W/TLR7-/-}$ (n=11), and $B^{W/TLR9-/-}$ (n=16), pooled from 4 independent experimental cohorts.
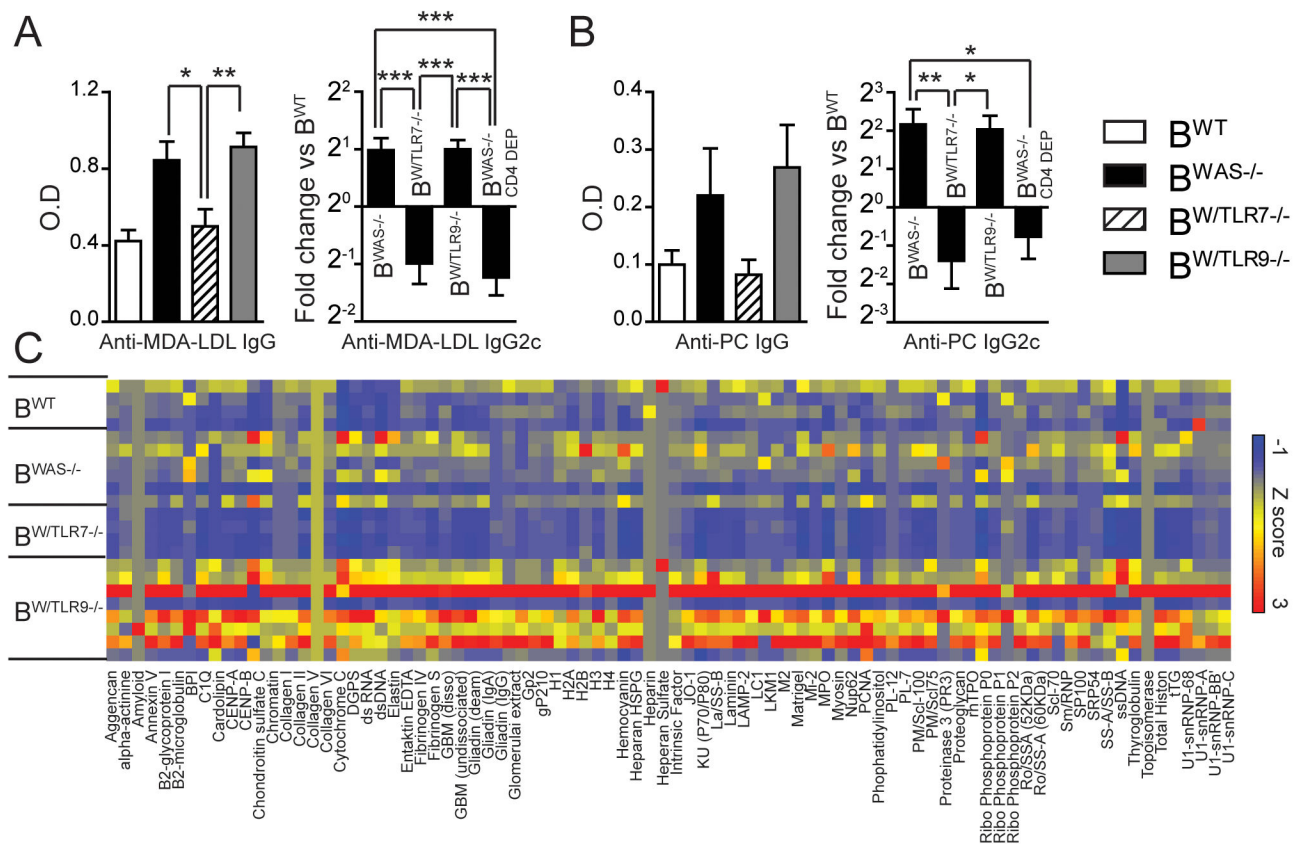
Figure 2. B cell-intrinsic TLR7 and TLR9 signals impact autoantibody reactivity to apoptotic and disease-associated antigens

(A) Left: Anti-MDA-LDL IgG. Right: Anti-MDA-LDL IgG2c in $B^{WAS-/-}$, $B^{W/TLR7-/-}$, $B^{W/TLR9-/-}$ and CD4-depleted $B^{WAS-/-}$ chimeras ($B^{WAS-/-}$ CD4 DEP). Data normalized to B^{WT} anti-MDA-LDL IgG2c titer. (B) Left: Anti-PC IgG. Right: Anti-PC IgG2c in $B^{WAS-/-}$, $B^{W/TLR7-/-}$, $B^{W/TLR9-/-}$ and CD4-depleted $B^{WAS-/-}$ chimeras ($B^{WAS-/-}$ CD4 DEP). Data normalized to B^{WT} anti-PC IgG2c titer. (A, B) Mean ± s.e.m. *, $P<0.05$; **, $P<0.01$; ***, $P<0.001$. Total mice analyzed: B^{WT} (n=7), $B^{WAS-/-}$ (n=13) $B^{W/TLR7-/-}$ (n=13), $B^{W/TLR9-/-}$ (n=14), and $B^{WAS-/-}$ CD4 DEP (n=10). (C) Serum IgG Abs from B^{WT} (n=4), $B^{WAS-/-}$ (N=6), $B^{W/TLR7-/-}$ (n=4) and $B^{W/TLR9-/-}$ (n=8) chimeras determined using an autoantibody array chip containing 88 specific autoantigens. Data are represented as a heat map of Z-scores ranging from −1 (blue) to 3 (red). Representative of two independent microarray analyses.
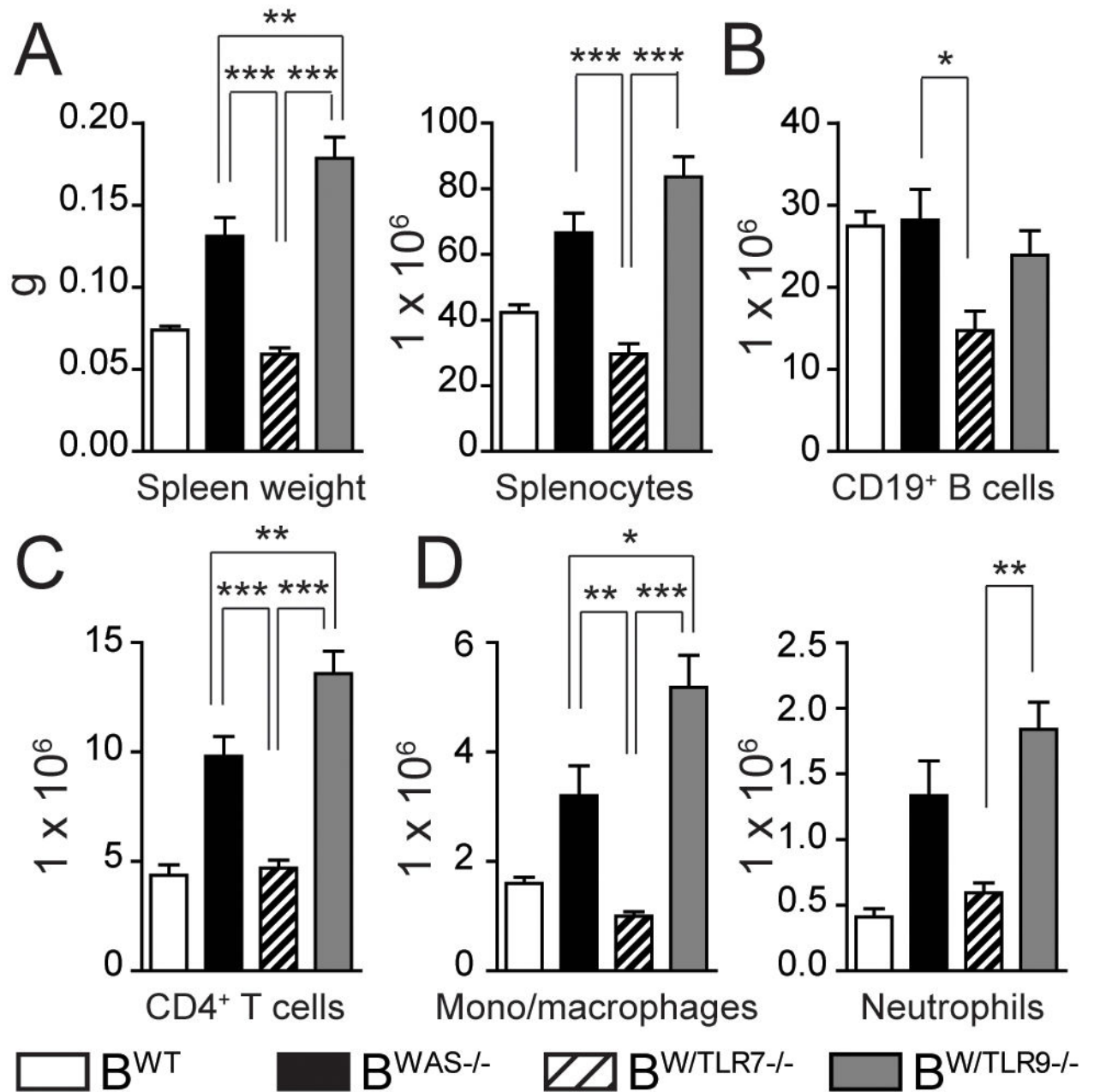
Figure 3. B cell-intrinsic TLR7 and TLR9 exert opposing signals on immune activation
Splenic monocyte subsets were analyzed in B^{WT}, $B^{WAS-/-}$, $B^{W/TLR7-/-}$ and $B^{W/TLR9-/-}$ chimeras at sacrifice. (A) Spleen weight and total splenocyte numbers. (B–D) Number of splenic: (B) $CD19^+$ B cells; (C) $CD4^+$ T cells; (D) $CD11b^+GR1^{LO}$ monocyte/macrophages and $CD11b^+GR1^+$ neutrophils. (A-D) Mean ± s.e.m. *, $P<0.05$; **, $P<0.01$; ***, $P<0.001$. Total mice analyzed: B^{WT} (n=5), $B^{WAS-/-}$ (n=12) $B^{W/TLR7-/-}$ (n=12), and $B^{W/TLR9-/-}$ (n=13), pooled from 4 independent experimental cohorts.
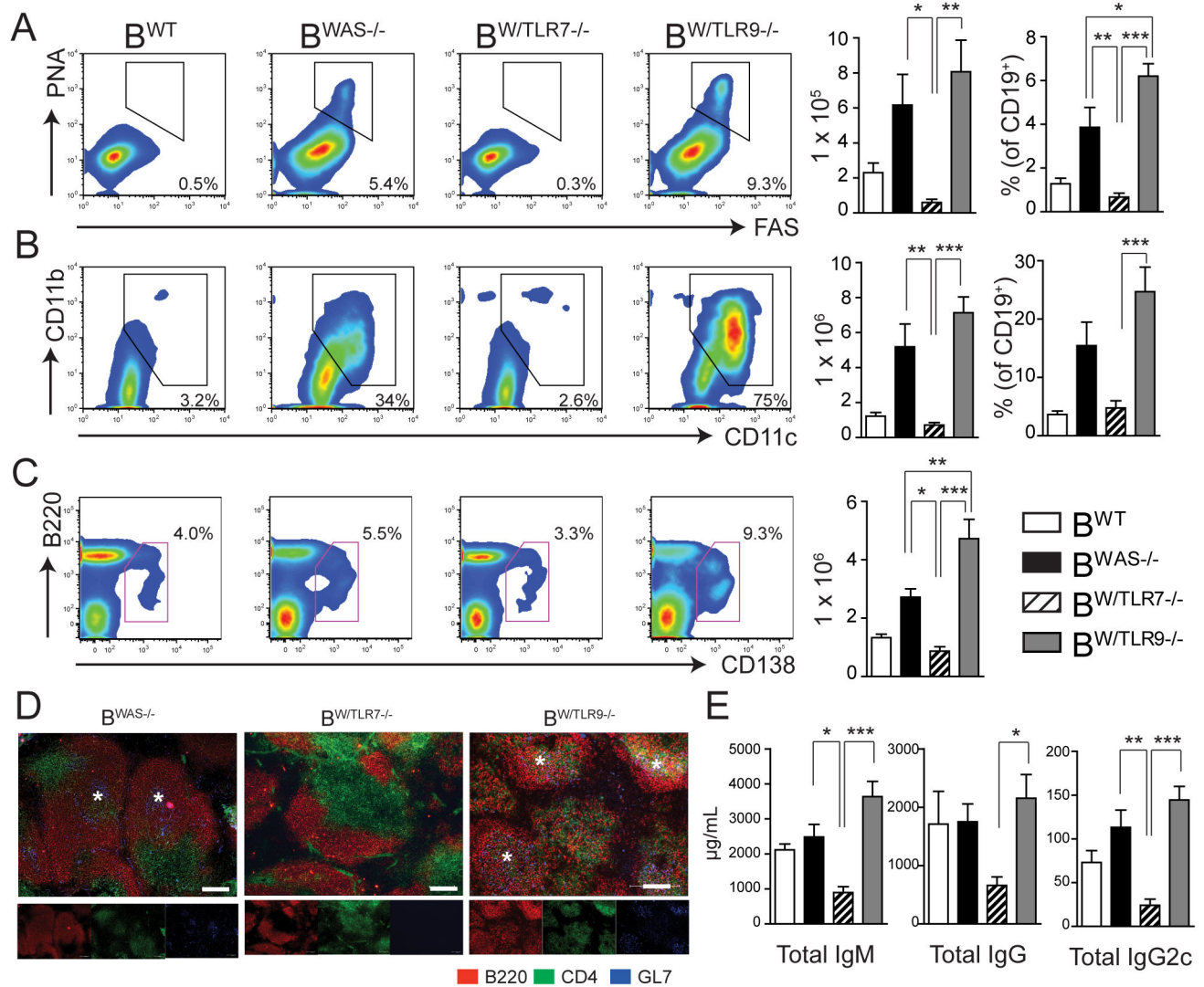
Figure 4. Divergent impact of B cell-intrinsic TLR7 and TLR9 on B cell activation

(A, B) Representative FACS plots (left), total number (middle) and percentage (right) of: (A) PNA$^+$ FAS$^+$ GL7$^+$ germinal center B cells (gated on CD19$^+$ B cells); and (B) CD11b$^+$ CD11c$^+$ "age-associated B cells" (gated on CD19$^+$ B cells). (C) Representative FACS plots (left) and total number (right) of B220^{LO} CD138$^+$ plasmablasts/plasma cells (gated on total splenocytes). (A–C) Number in FACS plot represents percentage within gated population. (D) Representative examples of splenic sections stained with B220 (red), CD4 (green) and GL7 (blue). Stars denote spontaneous GCs in B$^{WAS−/−}$ and B$^{W/TLR9−/−}$ chimeras (*). Images were taken with 10X objective: bars, 100μm. (E) Total IgM, IgG and IgG2c serum titers in B^{WT}, B$^{WAS−/−}$, B$^{W/TLR7−/−}$ and B$^{W/TLR9−/−}$ chimeras. (A–C, E) Mean ± s.e.m. *, $P<0.05$; **, $P<0.01$; ***, $P<0.001$. Total mice analyzed: B^{WT} (n=5), B$^{WAS−/−}$ (n=12) B$^{W/TLR7−/−}$ (n=12), and B$^{W/TLR9−/−}$ (n=13), pooled from 4 independent experimental cohorts.
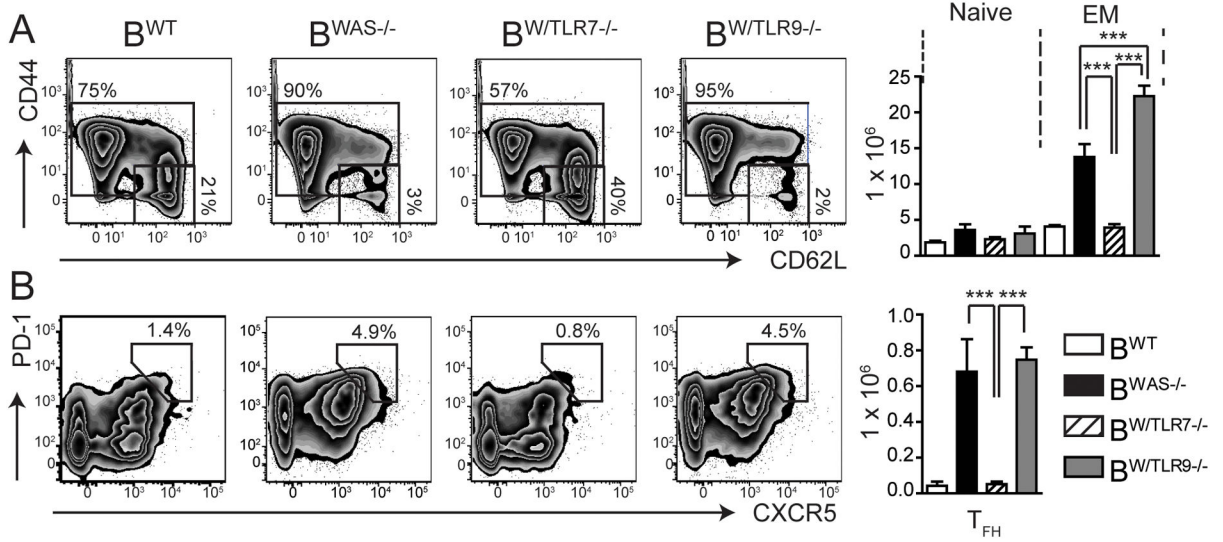
Figure 5. B cell-intrinsic TLR7 and TLR9 exert opposing impacts on T cell activation
(A, B) Representative FACS plots (left) and total number (right) of splenic: (A) naïve
(CD44^{LO}CD62L^{HI}) and effector/memory (EM; CD44^{HI}CD62L^{LO} and CD44^{HI}CD62L^{HI})
CD4$^+$ T cells; and, (B) PD1$^+$CXCR5$^+$ T follicular helper (T$_{FH}$) cells. Number represents
percentage within gated population (gated on splenic CD4$^+$ T cells). Mean ± s.e.m. ***,
$P<0.001$. Total mice analyzed: B^{WT} (n=5), B$^{WAS-/-}$, (n=12) B$^{W/TLR7-/-}$ (n=12), and
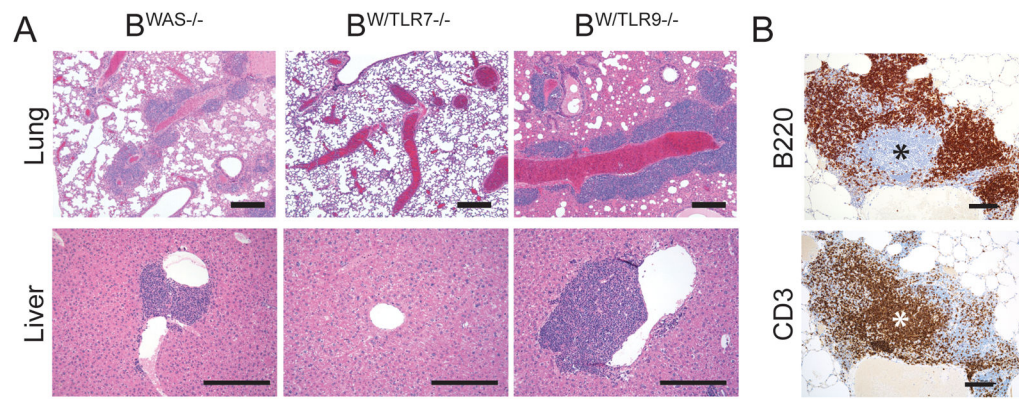B$^{W/TLR9-/-}$ (n=13), pooled from 4 independent experimental cohorts.

Figure 6. B cell-intrinsic TLR7 signals promote systemic inflammation and ectopic lymphoid follicles

(A) Hematoxylin and eosin (H&E) stained tissues sections showing prominent lymphoid aggregates surrounding pulmonary vasculature in the lungs (upper panels, 4X) and portal tracts of the liver (lower panels, 10X) in $B^{WAS-/-}$ and $B^{W/TLR9-/-}$ chimeras. Bars, 100μm. (B) Immunohistochemistry of serial lung sections from a representative $B^{W/TLR9-/-}$ mouse showing distinct B220$^+$ B cell follicle and CD3$^+$ T cell zone (*). Image taken with 10X objective. Bars, 100μm. (A, B) Data are representative of: B^{WT} (n=4), $B^{WAS-/-}$ (n=10), $B^{W/TLR7-/-}$ (n=9), and $B^{W/TLR9-/-}$ (n=11) mice, analyzed from 2 independent experimental cohorts.
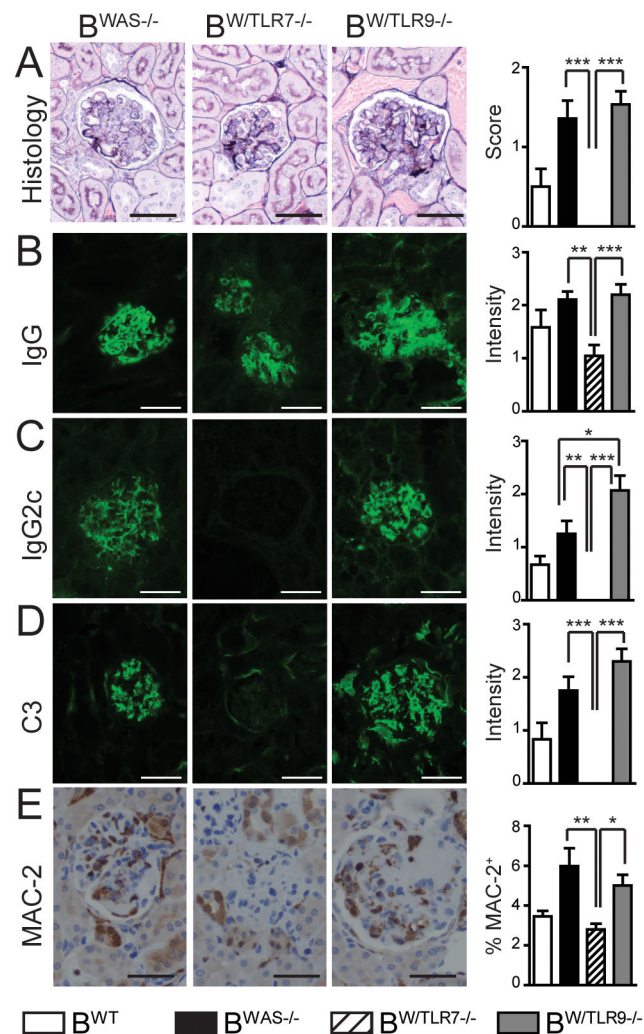
Figure 7. B cell-intrinsic TLR7 and TLR9 exert opposing effects on IC glomerulonephritis
(A) Left panels: Representative examples of glomeruli from $B^{WAS-/-}$, $B^{W/TLR7-/-}$ and $B^{W/TLR9-/-}$ chimeras stained with Jones' methenamine silver-Periodic acid-Schiff stain. Right panel: Glomerular inflammation scored as: (0+) minimal mesangial expansion consistent with radiation injury; (1+) focal glomerular changes with moderate mesangial expansion, GBM thickening/reduplication and glomerular hypercellularity; or, (2+) diffuse glomerular changes with severe mesangial expansion, GBM thickening/reduplication and glomerular hypercellularity. Pathology was scored by two observers blinded to genotype. (B–D) Glomerular immune-complex deposits were determined by immunofluorescence staining for: (B) IgG (C) IgG2c, and (D) complement C3. Representative images are shown (left), together with intensity of glomerular fluorescent staining (right) scored from 0–3+ by two independent, blinded observers. (E) Left panels: Representative images of immunohistochemistry staining for glomerular MAC-2$^+$ macrophages. Right panel: MAC-2$^+$ area as a percentage of total glomerular area determined using Image Pro Plus (Media Cybernetics, Inc.). 4 independent kidney sections were examined per mouse. Bars, 50μm. (A–E) Results are mean ± s.e.m. *, $P<0.05$; **, $P<0.01$; ***, $P<0.001$. Total mice

analyzed (A–D, E): B^{WT} (n=6, 4), $B^{WAS-/-}$ (n=14, 6), $B^{W/TLR7-/-}$ (n=11, 9), and $B^{W/TLR9-/-}$ (n=15, 8), from 3 (A–D) and 2 (E) independent experimental cohorts.